Permittivity characterization based on Radar Cross measurements

Etienne Perret

Permittivity characterization based on Radar Cross measurements

Etienne Perret, *Senior Member*, *IEEE*

(Invited Paper)

University of Grenoble Alpes, LCIS, F-26900, Valence, France
Institut Universitaire de France, F-75000, Paris, France
e-mail: etienne.perret@lcis.grenoble-inp.fr

***Abstract*— In this paper, classical radar approaches such as the ones recently introduced for chipless RFID identifications are used for nondestructive permittivity characterization of a large variety of materials. A metallic resonant scatterer is placed on the material to be characterized and thanks to the acquisition of its resonant frequency the permittivity can be directly extracted with the use of classical formulas. Simulation and measurement results are presented to show the potential of this characterization technique and to validate the concept.**

***Index Terms*— chipless RFID, radar, RCS, scatterer.**

I. INTRODUCTION

As the conventional RFID technologies, chipless RFID tags are also associated with a specific RF reader which is used to interrogate the tag and to capture the ID contained in it [1]. Most of the time, the incident wave is a UWB pulse which is able to meet the regulations. Processing the received signal - notably through a decoding step- can trace back to the information contained in the tag [1]-[3]. Chipless tags are fundamentally different from conventional RFID tags; they work without any communication protocol. They can be seen as targets with a specific radar signature, which can be interpreted in frequency or time domain. Chipless tags are most often made of resonant elements (frequency domain approach) or delay lines to produce a delay (time domain approach). A direct relationship between the geometry of each conducting element and the tag radar signature is to be found. These elements introduce distinctive signs into the EM tag footprint that will be used to encode the ID. These signs are typically peaks or dips in frequency (frequency domain approach) or in time (time domain approach) that we will be able to move by controlling a geometrical parameter of the tag. Fig. 1 shows an example of frequency tag, where the Radar Cross Section (RCS) of the tag is presented (Fig. 1 (b)). One can see the four peaks of resonance, each associated with a characteristic notch of the tag (Fig. 1). If we take the example of the time domain approach, the coding scheme implemented is exactly the one used in the SAW technology, the difference being that the chipless tag does not include any magneto-acoustic material, for cost reasons. In the received signal, it is the peak's positions that will partially allow the reading system to identify the tag uniquely.

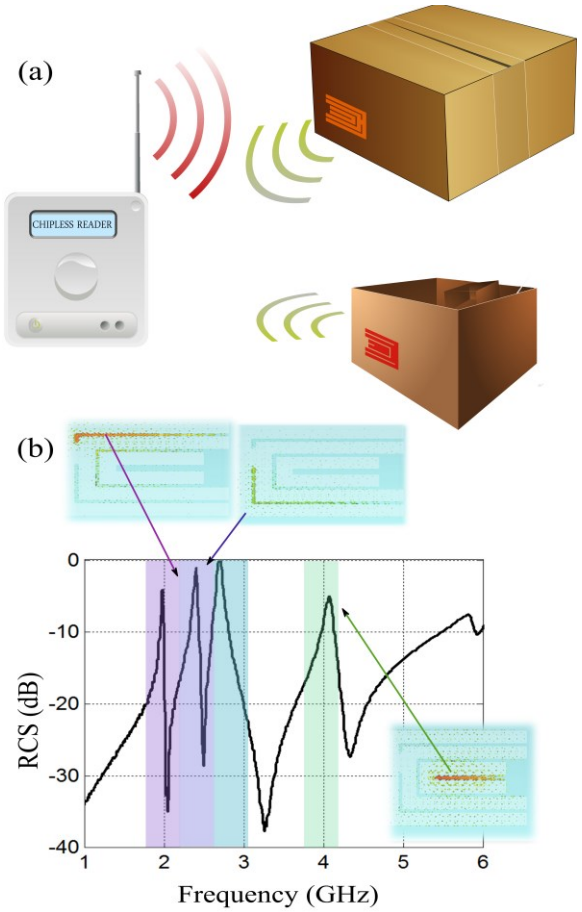

Fig. 1. (a) Operating principle of a chipless RFID system. (b) Illustration of the link that exists between the resonance frequencies and the geometry of C-shaped tags. Amplitude of the RCS or more simply the signal backscattered by the tag according to frequency.

Today, the RFID technology provides innovative solutions for applications in the domain of wireless sensing for physical parameters [4] due to the importance of this market. This technology is widely used and governed by well-established standards. In addition to the Identification function, classical RFID tags but also chipless RFID tags may also include sensor functions [5]-[7].

There are several measurement techniques existing for measuring dielectric properties of materials [8]-[10]. It is

because all of them are not appropriate for any kind nor any shape of materials. The most popular measurement techniques are:

- Coaxial probe method
- Resonant techniques
- Transmission line method
- Free space method
- Parallel plate capacitor method

Free space method has the advantage to be non-contacting and non-destructive. It is also a broadband technique where measurement at "any" frequency can be done. However, the calibration part of this method is challenging. Indeed the fact that this approach is "connector-less" induces special problems, especially regarding the difficulty to implement space calibration standards in practice. The material size can introduce errors from diffraction effects at the sample edges, and it is why the minimum frequency is set by the maximum practical sample length.

On the other hand, resonant techniques, like the cavity method, are accurate and well suited for low loss materials characterization [8], [9]. Calibration standards are much simple to realize in practice, and measurements are possible with small samples. However, measurements can be performed only at few frequencies and this technique requires a specific equipment, such as a cavity, which is expensive.

This paper deals with a preliminary work where a new measurement technique is introduced. The concept, based on a chipless RFID approach, is between resonant techniques and free space method. The technique rests on the use of a simple fully metallic resonant scatterer attached to the material to be characterized. As shown in Fig. 2, the system is composed of a fixed chipless RFID reader and a chipless tag positioned on the material under test, in the exact location where the measurement of the permittivity is planned. The permittivity is obtained from the measurement of the resonance frequency variation of each scatterer. Contrary to what is classically done in chipless RFID, no tag's substrate is needed, so that the resonant scatterer is directly in contact with the material under test, and no other uncertainty on the complex permittivity of the substrate is introduced in the measurement set up. A very simple resonant scatterer shape can be used and thanks to this, analytical expressions can be directly used to recover the permittivity form backscattered measurements (see Fig. 2). This resonant scatterer has a high Q factor and resonates at certain frequencies. Like resonant techniques, a sample of the material under test affects the resonant frequency and quality factor of the scatterer. The permittivity can be calculated from these parameters. This chipless based measurement technique is much less complex to implement in practice than the classic free space method, both in terms of calibration standards and of permittivity extraction for measurements results. As compared to resonant cavity methods, the adoption of fully metallic resonant scatterers in the measurement procedure reduces the cost of the system.

In the literature, a chipless RFID sensor has been recently introduced to detect the quality of materials in civil engineering [6]. For this, an ultra-wideband time-coded chipless tag has been developed, and the permittivity change can be detected by measuring the group delay of backscattering signal. In this article, we introduce a solution based on a frequency-coded chipless RFID tag, where the aim is to determine precisely the permittivity of materials.

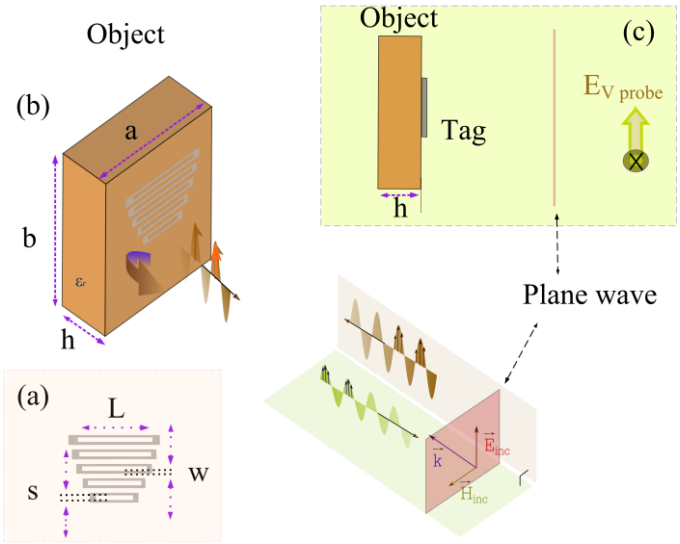

Fig. 2. Scheme of the tag-reader system for permittivity measurements and the transmitted and backscattered signals. (a) frequency-coded chipless RFID tag based on a loop shape. The tag is realized in Nickel, without any substrate, L= 35 mm, g= 0.5 mm, w=0.78 mm. (b) Simulation set up, configuration with the tag and the material under test (dielectric plate), a= 60 mm, b= 100 mm. (c). Side view of a tag behind the plate.

II. Basic Principle

A. Scattering

A chipless tag can be seen as a radar target that reflects part of the incident signal with its specific signature [1], [11]. A large number of scatterers based on a C-folded shape have been used in chipless RIFD [3], [12], [13]. The C-folded dipole has been identified among other single layer resonators [12] to have a good tradeoff in terms of RCS level and Q factor. A model based on coplanar strip-line (CPS) resonator is given in [13]. In this paper, a loop configuration is chosen (see Fig. 2(a)). The scatterer is also based on a CPS, and can thus be modeled like the classical C-shape. The difference is that the loop is a CPS with both sides as a short circuit. An accurate model for the computation of the resonance frequency f_r (1) based on well-known formula for CPS line can be used [14].

$$f_r = \frac{c}{2(L+\Delta L)\sqrt{\varepsilon_{reff}}} \qquad (1)$$

where L is the length of the slot, ΔL a supplementary length to take into account the fringing fields at the end of the transmission line, c the velocity of the light and ε_{reff} the effective relative permittivity of the CPS. ε_{reff} depends on the gap value s, the width W of the loop, as well as the substrate thickness h and permittivity ε_r [15]:

$$\varepsilon_{reff} = 1 + \frac{\varepsilon_r - 1}{2}\frac{K(k')K(k_1)}{K(k)K(k'_1)} \qquad (2)$$

K is the complete elliptic integral of the first kind and k, k' are both variables that can be expressed in terms of s, w and h. Note that, thanks to (2), ε_r can directly be derived from ε_{reff}

and the geometrical parameters of the CPS. By adjusting L, (1) enables to set the resonant frequency of a single scatterer with a loop shape. To extract the permittivity ε_r on a larger frequency band, several scatterers with different length L can be used as shown in Fig. 3.

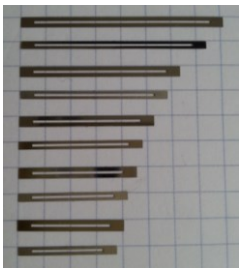

Fig. 3. Photograph of the tag used for permittivity characterization. The ten scatterers are made of nickel with a thickness of 150 µm.

B. Simulations

In order to prove the concept, a simulation was done using plane-wave excitation and E-field probes under CST Microwave Studio as depicted in Fig. 2(c). Three cases are considered: 1) scatterers plotted Fig. 3, simulated in free space, 2) scatterers applied on a Kapton film of 0.128 mm thickness ($\varepsilon_r = 3.56$, $tan\delta = 0.010$ at 3.275 GHz), 3) same thing on another dielectric slab of 1.95 mm thickness named Red test sample ($\varepsilon_r = 4.25$, $tan\delta = 0.018$ at 3.221 GHz). These two samples present a quite constant complex permittivity over the frequency range 0.8 GHz - 6 GHz. The backscattered E-field obtained by simulation is depicted in Fig. 4. By considering the free space (Air) configuration as a reference, (3) can be derived from (1):

$$\varepsilon_{reff}^{(i)} = \left(\frac{f_r^{(Air)}}{f_r^{(i)}}\right)^2 \qquad (3)$$

where i = {Kapton, Red}. Note that (3) can be applied to each frequency of resonance of the tag used for the characterization. Finally (4) can be obtained from (2) and (4):

$$\varepsilon_r^{(i)} = 2\left(\left(\frac{f_r^{(Air)}}{f_r^{(i)}}\right)^2 - 1\right)\cdot f(s,W,h) + 1 \qquad (4)$$

where $f(s,W,h) = \frac{K(k)K(k'_1)}{K(k')K(k_1)}$.

Thus the extraction of the effective relative permittivity and the relative permittivity ε_r can be done respectively by using (3) and (4). These expressions have been used for the two test samples simulated in Fig. 4. The results are given in table 1. One can notice that the results show a good agreement.

III. Design Validation – Measurement Results

The frequency measurement setup used is the same as the one previously introduced in [13]. A photograph of the measurement environment for the tag placed on a kapton film is presented in Fig. 5. The antenna used is a SATIMO QH2000 (open boundary wideband quad ridge antenna) dual polarization that operates in the 2–32-GHz band. Its gain is between 6–11 dBi between 2–10 GHz. As shown in Fig. 5, a bi-static radar configuration is used. The S_{21}-parameter at the VNA provides the tag response in co-polarization.

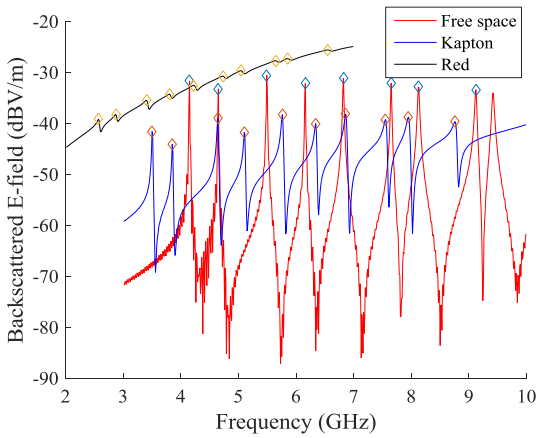

Fig. 4. Simulation results (CST) of the backscattered E-field of the ten loop shape scatterers used of permittivity extraction. The peak apex corresponding to the frequencies of resonance f_r of the loops are plotted for different configurations: 1) free space, 2) tag applied on Kapton film, 3) tag applied on Red test sample.

TABLE 1 – Results of the extraction of the effective relative permittivity ε_{reff} and the relative permittivity ε_r

Configurations – sample under test	ε_{reff} (3)	ε_r (4)
Kapton (reference- Cavity measurements), 3.275 GHz	1.40 with (2)	3.56
Red (reference - Cavity measurements), 3.221 GHz	2.58 with (2)	4.25
Kapton (Simulations Fig. 4)	1.45	3.84
Red (Simulations Fig. 4)	2.58	4.26
Kapton (Measurements Fig. 6)	1.37 with (3) | 1.35 with [16]	3.74 with [16]
Red (Measurements Fig. 6)	2.08	3.81

The tag is alternately attached to the foam, the Kapton film and the Red test sample. The tag is measured at a 35 cm tag-reader distance, and its response is shown in Fig. 6 for the three configurations. Note that the tag is not in free space as simulated, but placed on a foam that can be seen Fig. 5. Comparing Fig. 6 with Fig. 4, it is clear that this foam cannot be considered as a material with permittivity of 1. The introduced methodology has been used to extract the permittivity of the foam (the frequencies of reference are the ones obtained from the simulation), and a value of 1.20 has been obtained.

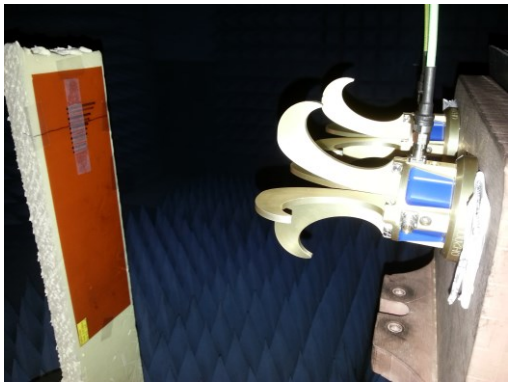

Fig. 5. Photograph of the tag applied on a Kapton film in the anechoic chamber.

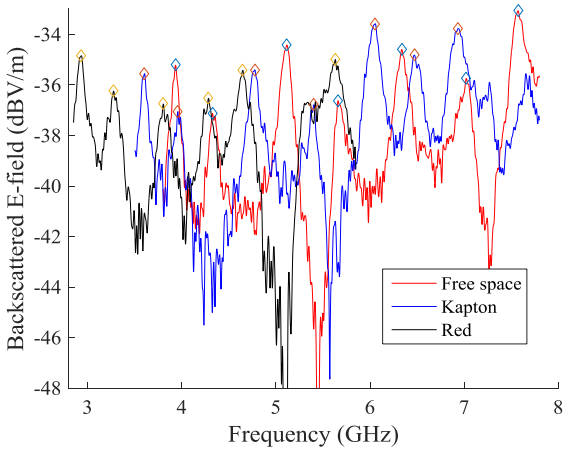

Fig. 6. Measurement results of the backscattered E-field of the ten loop shape scatterers used for permittivity extraction. The peak apex corresponding to the frequencies of resonance f_r of the loops are plotted for different configurations: 1) free space, 2) tag applied on Kapton film, 3) tag applied on Red test sample.

This means that a more complex model, taking into account the presence of two layers [16] has to be used to extract the permittivity. A simpler technique will consist in doing measurements again without any foam. The latter approach will be done in a further work. Because of the presence of this foam, measurement results presented in table 1 show a lower agreement than expected. Anyway, these results confirm the possibility of doing permittivity measurements with this chipless RFID based method. As previously explained, to estimate the material permittivity ε_r on a larger frequency band, it is possible to use all the scatterers (see Fig. 3). This will be done in a further work.

IV. Conclusion

In this paper, we introduced a new measurement technique of dielectric slab permittivity, based on a chipless RFID approach. Further works have to be done to show the entire potential of this approach. For example, a more elaborated technic based on the short-time Fourier transform could be used to extract the material losses, thanks to the derivation of the Q factor of each scatterer.

Acknowledgment

The Author would like to thank Dr A. Ramos and O. Rance, University of Grenoble Alpes - LCIS, for their assistance.

References

[1] E. Perret, Radio Frequency Identification and Sensors: From RFID to Chipless RFID: Wiley-ISTE, 2014.

[2] R. Rezaiesarlak and M. Manteghi, Chipless Rfid: Design Procedure and Detection Techniques: Springer, 2014.

[3] A. Vena, E. Perret, and S. Tedjini, "Chipless RFID tag using hybrid coding technique," IEEE Transactions on Microwave Theory and Techniques, vol. 59, pp. 3356-3364, 2011.

[4] C. Occhiuzzi, S. Caizzone, and G. Marrocco, "Passive UHF RFID antennas for sensing applications: Principles, methods, and classifcations," IEEE Antennas and Propagation Magazine, vol. 55, pp. 14-34, 2013.

[5] D. Girbau, A. Ramos, A. Lazaro, S. Rima, and R. Villarino, "Passive Wireless Temperature Sensor Based on Time-Coded UWB Chipless RFID Tags," IEEE Transactions on Microwave Theory and Techniques, vol. 60, pp. 3623-3632, 2012.

[6] A. Ramos, A. Lazaro, and D. Girbau, "Time-coded chipless sensors to detect quality of materials in civil engineering," 9th European Conference on Antennas and Propagation (EuCAP), 2015, pp. 1-4.

[7] R. S. Nair, E. Perret, S. Tedjini, and T. Baron, "A Group Delay Based Chipless RFID Humidity Tag Sensor Using Silicon Nanowires," IEEE Antennas and Wireless Propagation Letters, vol. 12, pp. 729-732, 2013.

[8] Basics of Measuring the Dielectric Properties of Materials. Agilent Technologies - Application note, Literature number 5989-2589EN.

[9] L. F. Chen, C. K. Ong, C. P. Neo, V. V. Varadan, and V. K. Varadan, "Microwave Theory and Techniques for Materials Characterization," Microwave Electronics, John Wiley & Sons, 2005, pp. 37-141.

[10] E. Fratticcioli, M. Dionigi, and R. Sorrentino, "A simple and low-cost measurement system for the complex permittivity characterization of materials," IEEE Transactions on Instrumentation and Measurement, vol. 53, pp. 1071-1077, 2004.

[11] A. Vena, E. Perret, and S. Tedjini, "A Depolarizing Chipless RFID Tag for Robust Detection and Its FCC Compliant UWB Reading System," IEEE Transactions on Microwave Theory and Techniques, vol. 61, pp. 2982 - 2994, 2013.

[12] A. Vena, E. Perret, and S. Tedjini, "Design Rules For Chipless RFID Tags Based on Multiple Scatterers," Annals of telecommunications, special issue on Chipless RFID, feb. 2013.

[13] A. Vena, E. Perret, and S. Tedjini, "Design of Compact and Auto Compensated Single Layer Chipless RFID Tag," IEEE Transactions on Microwave Theory and Techniques, vol. 60, pp. 2913 – 2924, Sep. 2012.

[14] J. L. Narayana, K. S. R. Krishna, and L. P. Reddy, "ANN models for coplanar strip line analysis and synthesis," International Conference on Recent Advances in Microwave Theory and Applications, 2008, pp. 682-685.

[15] G. Ghione and C. Naldi, "Analytical formulas for coplanar lines in hybrid and monolithic MICs," Electronics Letters, vol. 20, pp. 179-181, 1984.

[16] S. Gevorgian and H. Berg, "Line Capacitance and Impedance of Coplanar-Strip Waveguides on Substrates with Multiple Dielectric Layers," 31st European Microwave Conference, 2001.